Available online at www.sciencedirect.com
SCIENCE DIRECT®
Experimental Thermal and Fluid Science 27 (2003) 705–713
Experimental Thermal and Fluid Science
www.elsevier.com/locate/etfs

Convective boiling of R-407c inside horizontal microfin and plain tubes

Júlio César Passos [a,*], Vinicius Fernando Kuser [a], Phillipe Haberschill [b], Monique Lallemand [b]

[a] Departamento de Engenharia Mecânica, Universidade Federal de Santa Catarina, LABSOLAR-NCTS, Florianópolis, SC 88010-970, Brazil
[b] Centre de Thermique de Lyon, Institut National des Sciences Appliquées de Lyon-UMR-CNRS, 5008, 20, Av. Albert Einstein, 69621 Villeurbanne cedex, France

Received 18 February 2002; received in revised form 15 September 2002; accepted 24 October 2002

Abstract

This work presents experimental results on the nucleate and convective boiling of R-407c, flowing with a mass velocity in the range 200–300 $kg\,m^{-2}\,s^{-1}$, at 770 kPa, inside horizontal plain and microfin tubes with outside diameters (OD) of 7.0 and 12.7 mm. The data are presented for heat fluxes of 10 and 20 $kW\,m^{-2}$. The experimental data are discussed in terms of the heat transfer coefficient and the pressure drop as a function of the vapor quality. For a heat flux of 10 $kW\,m^{-2}$ and a mass velocity of 200 $kg\,m^{-2}\,s^{-1}$, the dominant heat transfer mechanisms for the 7 mm OD tube is the nucleate boiling regime whereas for the 12.7 mm OD tube it is the convective boiling regime.

Keywords: Convective boiling; Enhanced surface; Nucleate boiling; Dryout; Microfin tube; R-407c

1. Introduction

The important role of two-phase forced flow in the modern heat exchanger industry and the political decision to phase out chlorofluorocarbons (CFCs) due to their high ozone depletion potential (ODP) [1] along with the scheduled phase out of hydrochlorofluorocarbons (HCFCs), particularly R-22, has prompted several laboratories to analyze the behavior of new refrigerants flowing inside tubes. R-22 is largely employed in the industrial refrigeration field and although it has a low ODP (0.055), compared to the unit value for R-12; it is necessary to consider the large amount of R-22 that commonly escapes from commercial units to the atmosphere and can arrive at the stratosphere where the chlorine can combine with ozone [1]. The hydrofluorocarbons (HFCs), such as R-32, R-125 and R-134a, contain no ozone-depleting chlorine. However, CFCs, HCFCs and HFCs exhibit a certain global-warming potential (GWP). The GWP for R-32, R-125 and R-134a are equal to 0.12, 0.63 and 0.31, respectively [1].

Among the new refrigerants the one currently accepted to replace R-22 is R-407c which is a ternary zeotropic mixture of R-32, R-125 and R-134a, whose main thermodynamic properties are very close to those of R-22 [2,3] allowing the utilization of this mixture in existing machinery without major modifications. Zeotropic mixtures are characterized by differences between the bubble and the dew points. The more volatile components are converted into vapor first and the liquid phases, therefore, become richer in the less volatile components which is the cause of the gliding temperature during boiling [4]. The depletion of the more volatile components causes an increase in the local saturation temperature in the liquid layer near the heating wall [5], and is responsible for the decrease in the heat transfer coefficient for a pool boiling of refrigerant mixtures. For convective boiling systems a similar behavior can be observed in the region of nucleate boiling

* Corresponding author. Tel.: +55-48-331-9379; fax: +55-48-234-15-19.
E-mail address: jpassos@emc.ufsc.br (J.C. Passos).

0894-1777/03/$ - see front matter © 2003 Elsevier Science Inc. All rights reserved.
doi:10.1016/S0894-1777(02)00308-4

Nomenclature

CFC	chlorofluorocarbon
d, ID	inside diameter, m
Fr	Froude number
g	acceleration due to gravity, $m\,s^{-2}$
G	mass velocity, $kg\,m^{-2}\,s^{-1}$
h	heat transfer coefficient, $W\,m^{-2}\,K^{-1}$
h_{fg}	latent heat of vaporization, $J\,kg^{-1}$
$\overline{h_{mf}}$	average heat transfer coefficient for microfin tube, $W\,m^{-2}\,K^{-1}$
$\overline{h_p}$	average heat transfer coefficient for plain tube, $W\,m^{-2}\,K^{-1}$
l	length of the test section, m
N	number of rib starts
$\overline{\Delta p_{mf}}$	average pressure drop gradient for microfin tube, Pa
$\overline{\Delta p_p}$	average pressure drop for plain tube, Pa
q	heat flux, $W\,m^{-2}$
T	temperature, K
x	quality
z	distance from the entrance of the test section, m

Greek Letters

β	helix angle
δ	fin height, m, mm
γ	angle between sides of ribs
η	efficiency index
ρ	density

Subscripts

bp	bubble point
dp	dew point
l	liquid
mf	micro finned
p	plain
sat	saturation
v	vapor
w	wall

as described by Celata et al. [6]. In order to compensate for the reduction in the heat transfer coefficient caused by the simple replacement of a pure fluid by a zeotropic mixture containing the pure fluid flowing in commercial plain tubes, new enhanced tubes can be used whose inside surfaces are finned [7,8].

The most common commercial evaporators are those in which the refrigerant boils inside the tubes [9]. At higher vapor qualities the forced flow boiling inside a tube tends towards an annular regime, known as convective boiling [10,11] which is characterized by a liquid film around the tube perimeter and a vapor core. At the first part of the flow vapor bubbles are created inside the superheated liquid film and the nucleate boiling regime becomes the dominant heat transfer mechanism and this mechanism tends to be progressively reduced due to a decrease in the film thickness and the wall temperature. The second part of the flow is characterized by the elimination of nucleate boiling due to the liquid film being very thin and the wall temperature not being sufficiently high to sustain nucleate boiling [12]. At the same time the forced convective mechanisms of heat transfer, without vapor bubbles, become dominant and vaporization occurs at the interface of the liquid film and the vapor core by conduction heat transfer through the liquid film.

This work is a continuation of a previous study, [13], and it presents the experimental results, at a pressure of 770 kPa, for a two-phase forced flow, including nucleate boiling and convective boiling, of the zeotropic mixture R-407c inside horizontal plain and microfin tubes with outside diameters (OD) of 7 and 12.7 mm. The heat transfer and pressure drop coefficients and the dryout phenomenon will be considered.

2. Literature review

The objective of this review is to characterize the main trends found in heat transfer and pressure drop research using zeotropic mixtures with convective boiling and to compare the results with pure refrigerants.

2.1. Effects of the mass velocity and working fluid

Chamra et al. [14] analyzed the effect of the mass velocity ($G = 72$–$289\ kg\,m^{-2}\,s^{-1}$) for an R-22 flow inside horizontal tubes, plain and micro-finned, with OD = 15.88 mm (inside diameter, ID = 14.87 mm). They showed that the heat transfer enhancement ratio (h_{mf}/h_p), where h_{mf} and h_p represent the experimental heat transfer coefficients for microfin and plain tubes, respectively, vary between 1.70 and 4.56, and decrease when the value of G increases. These authors also studied the effect of the mass velocity on the pressure drop ratio ($\Delta p_{mf}/\Delta p_p$), where Δp_{mf} and Δp_p represent the pressure drop for microfin and plain tubes, respectively. They found that ($\Delta p_{mf}/\Delta p_p$) varies between 1.38 and 1.93 and the performance index $((h_{mf}/h_p)/(\Delta p_{mf}/\Delta p_p))$ varies between 1.03 and 3.00 and decreases when G increases.

Kuo and Wang [15] determined the heat transfer coefficients and the pressure gradients for boiling of

R-22 and R-407c, at 600 kPa, in forced convection inside a horizontal microfin tube (OD = 9.52 mm), for G and heat flux in the ranges 100–300 $kg\,m^{-2}\,s^{-1}$ and 6–14 $kW\,m^{-2}$, respectively. They found that the heat transfer coefficient for R-407c is 50–80% less than that for R-22. The pressure gradient of R-407c is 30–50% lower than that for R-22. For a fixed heat flux the heat transfer coefficient increases with an increase in the mass velocity for both fluids. However, this general trend was not so clear for R-407c, for a heat flux of 10 $kW\,m^{-2}$ and mass velocities of 100 and 200 $kg\,m^{-2}\,s^{-1}$, due to the small differences in the heat transfer coefficients; a clear effect of the influence of G was observed only when $G = 300$ $kg\,m^{-2}\,s^{-1}$. The authors also considered the hypothesis that flow configurations for R-22 and R-407c under the same test conditions are not the same, which can explain some of the differences in the pressure gradients and in the heat transfer coefficients.

Lallemand et al. [13] presented experimental results obtained by Branescu [16] for R-22 and R-407c, at 770 kPa, flowing inside horizontal plain (ID = 10.70 mm) and microfin (ID = 11.98 mm) tubes, with OD = 12.70 mm. The heat transfer coefficients for microfin tubes are 110–170% higher than those for plain tubes. For R-407c the average heat transfer coefficients are 15–75% and 20–35% less than those for R-22 with the plain and microfin tubes, respectively.

2.2. Nucleate and convective boiling regimes

Ross et al. [17] analyzed the behavior of the boiling forced flow of three pure refrigerants (R-152a, R-22 and R-13B1) and four zeotropic mixtures of R-152a and R-13B1 inside a horizontal plain stainless steel tube with 2.7 m length and 9.0 and 9.5 mm inside and outside diameters, respectively. The results suggest that the nucleate boiling suppression is easier to achieve with mixtures than pure fluids. For pure refrigerants the experiment results show a higher heat transfer coefficient at the top than in the middle and at the bottom of the tube wall because the liquid film at the top is thinner than at the bottom and in the middle due to gravity. For mixtures the heat transfer coefficient at the tube bottom is higher than at the top and five hypothesis are presented to explain this contrary behavior for mixtures including the possibility of there being different flow patterns in mixtures compared with pure fluids, different concentrations at the bottom and at the top of the tube and nucleate boiling at the bottom of the tube, but not at the top.

2.3. Geometrical effects

Seo and Kim [18] compared the heat transfer enhancement effect for R-22 inside in microfin tubes with OD = 7 and 12.7 mm and showed that the heat transfer is more effective in the larger diameter tubes. However, for plain tubes under the same test conditions they found that the heat transfer coefficient, for a fixed value of vapor quality, is less for a tube diameter of 12.7 than for 7 mm. Seo and Kim [18] explained this inversion of results by the fact that the fins promote an effect of convective boiling.

Results reported by Klimenko [19,20] show that the heat transfer coefficient for convective boiling of pure substances inside smooth tubes is not so dependent on the tube diameter.

Four fin geometries of the internal helical of microfin tubes were analyzed by Chamra et al. [14] for an R-22 flow inside a tube of 15.87 mm outside diameter. These authors concluded that the maximum heat transfer coefficient occurs at a 20° helix angle for all the tested geometries.

2.4. The flow stratification

In a horizontal two-phase flow it is important to verify the order of magnitude of the ratio between the inertia and gravitational forces which is represented by the modified vapor Froude number, given by the following equation:

$$Fr_v = \frac{(Gx)^2}{\rho_v(\rho_l - \rho_v)gd} \tag{1}$$

This equation shows that the Fr_v decreases with an increase of the tube diameter. Stephan [4] has reported the results presented by Wallis [21] that if Fr_v is higher than 49 there is no stratification, whereas for Fr_v less or equal to 9 the stratification is pronounced. Liu and Winterton [22] considered that the stratification in a horizontal flow inside a tube occurs when the liquid Froude number, given by the following equation, is less than 0.05:

$$Fr_l = \frac{G^2}{\rho_l g d} \tag{2}$$

2.5. The dryout phenomenon

The contact interruption of the liquid film in an annular flow is known as the dryout phenomenon, and it is attributed to the effect of evaporation and hydrodynamic forces that cause the entraining of droplets from the liquid film [10]. In heat flux controlled systems, the beginning of dryout is accompanied by a decrease in the heat transfer coefficient and, consequently, by an increase in the wall temperature. Therefore, a knowledge of dryout is necessary because it represents the limit of good performance for boiling heat transfer in convective boiling.

Very few studies on dryout inside microfin tubes can be found in the literature. Mori et al. [23] presented results on the dryout quality for smooth and microfin

tubes and post dryout heat transfer coefficients for HFC-134a and HCFC-22 in horizontal tubes. Their experimental results show that the dryout qualities depend strongly on the mass velocity G and heat flux q. For the microfin tubes the dryout qualities at high G and high q are higher than those in plain tubes.

3. Experimental apparatus and procedure

3.1. The test section

Fig. 1 shows the scheme of the test section. This horizontal test section is part of a loop [13,16], that allows testing of R-22 and R-407c on boiling in forced convection and it consists of the following main elements: a pump, a mass flow-meter, a pre-heater (power of 9 kW), the test section, a condenser, a storage tank (capacity of 5.8 l) and a cooler. The loop pressure is controlled in the condenser by means of a water–glycol flow with a temperature between −5 and 8 °C, depending on the test conditions.

The test section has a length of 1.5 m and the evaporator tube is heated by contact with two halves of a brass shell, in turn heated by a second brass shell, on which twelve electrical resistances are inserted, as shown in Fig. 1, and finally thermally insulated by using *a 50 mm thickness of glass wool*. The test zones are located in the last 0.50 m of the test section, where there are three instrumented sections, at $z_1 = 1.00$ m, $z_2 = 1.17$ m and $z_3 = 1.34$ m, where z_1, z_2 and z_3 represent the distance from the entrance of the test section, noted as sections A, B and C, respectively in Fig. 1. Each of these sections are instrumented with two insulated type K (chromel–alumel) thermocouples of 0.5 mm diameter, one at the top and the other one at the bottom, as shown in Fig. 1. The contact of the thermocouples with the outside wall of the evaporator tube is assured by a thermal paste and by pressing the brass shell against the evaporator tube. Two other thermocouples are placed at the beginning and the end of the test section in the center of the flow. The typical uncertainty of each thermocouple is ±0.1 K.

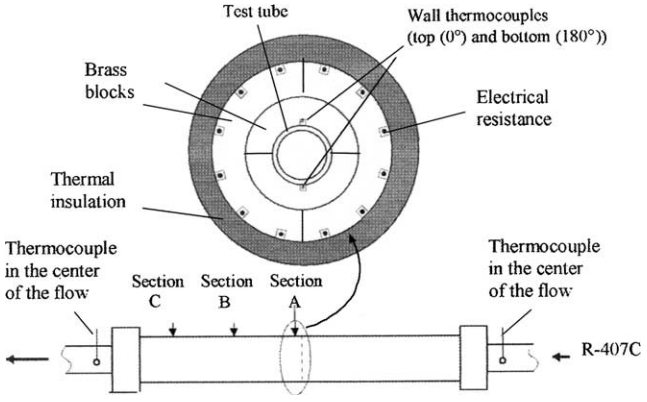

Fig. 1. Scheme of the test section.

A differential pressure transducer allows the measurement of the pressure drop between the extremities of the test section by means of a DC electrical current in the range of 4–20 mA. The precision of the differential pressure transducer is ±0.5% for measurements in the range of 0–60 kPa. The absolute pressure at the end of the test section is measured by means of a membrane transducer that associates an electrical signal of 4–20 mA to the membrane deformation, the uncertainty of which is ±1% for the scale of 20 bar.

All the evaporator tubes are made of copper and their geometry dimensions are summarized in Table 1, where the outside and the inside diameters, the number of fins (N), the twist angle (β), the angle between sides of the ribs (γ), the height of the ribs (δ) and the ratio (ES) between the inside surface area of a microfin tube and the inside surface area of a plain tube, computed as a function of the maximum diameter (to root of the ribs), are given.

3.2. The fluid properties

The composition by weight of the zeotropic R-407c mixture is 23% of R32, 25% of R125 and 52% of R134a

Table 1
Tube geometry

Tube	OD (mm)	ID (mm)	N	β (deg)	γ (deg)	δ (mm)	ES
Smooth	7.00	6.5	–	–	–	–	1.00
Smooth	12.70	10.70	–	–	–	–	1.00
Finned	7.00	6.48	50	18	50	0.15	1.46
Finned	12.70	11.98	65	30	65	0.25	1.48

Table 2
Physical properties of R-407c at 770 kPa

Components (% weight)	T_{bp} (°C)	T_{dp} (°C)	h_{fg} (kJ kg^{-1})	σ (N m^{-1})	c_p (kJ kg^{-1} K^{-1})	ρ_l (kg m^{-3})	ρ_v (kg m^{-3})
R32/R125/R134a 23%/25%/52%	9.76	15.62	201.15	0.00918	1448	1200	32.81

[1]. Table 2 presents the thermodynamical properties of R-407c calculated by REFPROP property routine, Version 6.0 developed at NIST [24]. The non-variation of the nominal composition of the R-407c samples was checked by chromatography before and after some tests.

3.3. Data reduction

The experimental heat transfer coefficients were computed as follows:

$$h = \frac{q}{(T_w - T_{sat})} \tag{3}$$

where q is the heat flux and T_w represents the average inner tube wall temperature which was computed using the Fourier equation by means of the outer wall temperature of the evaporator tube measured at two points, at the top and at the bottom, as shown in Fig. 1. T_{sat} represents the refrigerant bulk temperature, calculated from linear interpolation of the measured temperatures, at the center axis of the flow at the beginning and the end of the evaporator tube. This hypothesis is acceptable because the maximum variation in the quality is equal to 0.2 per meter of the evaporator. The definition of h, given by Eq. (3), as a function of $(T_w - T_{sat})$, was also employed by Celata et al. [6], Zhang et al. [25], Seo and Kim [18] and Lallemand et al. [13]. It differs from that presented by Carey [11], in which T_{sat} was replaced by the temperature of the bubble point of the mixture, T_{bp}. The latter was employed by Kuo and Wang [15], Kattan [26] and Kattan et al. [27].

The average heat transfer coefficient for the microfin tube was computed by

$$\overline{h_{mf}} = \frac{1}{(x_n - x_0)} \sum_{i=1}^{n} \frac{(h_{mf_i} - h_{mf_{i-1}})}{2} (x_i - x_{i-1}) \tag{4}$$

A similar equation was used for the plain tube.

The average pressure drop for the microfin tube was computed by

$$\overline{\Delta p_{mf}} = \frac{1}{(x_n - x_0)} \sum_{i=1}^{n} \frac{(\Delta p_{mf_i} - \Delta p_{mf_{i-1}})}{2} (x_i - x_{i-1}) \tag{5}$$

A similar equation was used for the plain tube.

The efficiency index [14] is defined as

$$\eta = \frac{\dfrac{\overline{h_{mf}}}{h_p}}{\dfrac{\overline{\Delta p_{mf}}}{\Delta p_p}} \tag{6}$$

3.4. Procedure

The chosen test conditions were in the following ranges: the mass velocities were between 100 and 300 $kg\,m^{-2}\,s^{-1}$, the heat fluxes were between 10 and 20 $kW\,m^{-2}$, the pressure was fixed at 770 ± 15 kPa, and the vapor quality varied between 0 and 1.0. The time required to stabilize the system after any change in the test conditions was 30 to near 90 min.

In order to have, for each test condition, minimal differences in the qualities of the three measurement sections the vapor quality was limited to 0.2 per meter in the evaporator tube and was computed by the following equation:

$$\Delta x = \frac{4ql}{Gh_{fg}d} \leqslant 0.2 \tag{7}$$

where l is the length of the evaporator tube and h_{fg} represents the latent heat of vaporization. The test matrix was then determined by this criterion.

3.5. Experimental uncertainty

The experimental uncertainties were computed following the procedures presented by Kline [28] and Holman [29]. The average temperature of the electrical resistances are very close to the laboratory temperature and the heat lost across the insulation is less than 0.3%. The standard deviation for the difference in the $(T_w - T_{sat})$ is 0.13 K, and the corresponding experimental uncertainty is ± 0.26 K. The experimental uncertainty of the heat flux is $\pm 1.4\%$. The maximum experimental uncertainty of G is 2%. The experimental uncertainty for the heat transfer coefficient for the tube with OD = 12.7 mm varied between $\pm 3.7\%$ and 6.6% whereas for the tube with OD = 7 the maximum value was $\pm 8.5\%$.

4. Results and discussion

4.1. Characterization of the flow regime

Fig. 2 shows the variation in the vapor Froude number, for each diameter of plain tubes, as a function

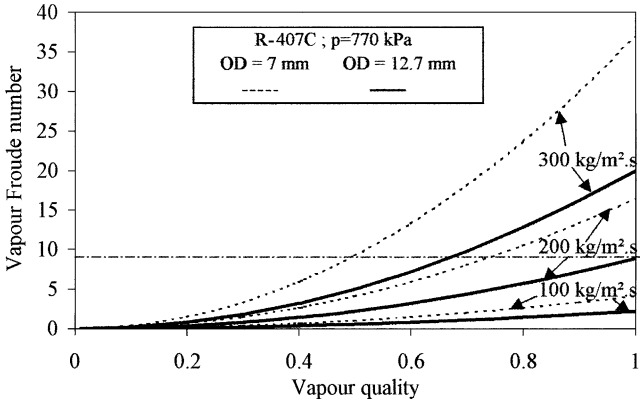

Fig. 2. Vapor Froude number for the test conditions.

Table 3
Froude number for liquid and vapor

ID (mm)	G ($kg\,m^{-2}\,s^{-1}$)	Fr_l	Fr_v ($x = 0.50$)	Fr_v ($x = 0$; $x = 1$)
6.48	100	0.1	1.0	0–4.1
	200	0.4	4.1	0–16.4
	300	1.0	9.2	0–37.0
11.98	100	0.1	0.6	0–2.2
	200	0.2	2.2	0–8.9
	300	0.5	5.0	0–20.0

of the vapor quality for R-407c. For the majority of the test conditions for OD = 12.7 mm the Fr_v is less than 9 whereas for OD = 7 mm the Fr_v is higher than this value. However, for all test conditions used in this work the vapor Froude number is not higher than 49, which would represent, from our literature review, the condition of a non-stratified flow. Table 3 shows the values of Fr_v and Fr_l. Only limiting our analysis to the values of Fr_l, as was considered by Liu and Winterton [22], the flow can be considered not stratified. The analysis of the present test conditions inside smooth tubes of 6.5 and 10.7 mm inner diameters and with heat fluxes of 10 and 20 kW/m^2, for R-407c and R-22, using the flow pattern map as proposed by Kattan [26] and Kattan et al. [27] shows that the flow regime is annular or intermittent and for a quality higher than 0.35–0.4 the regime is annular. Therefore, the results that will be presented in the following sections can be considered as representative of non-stratified flows because of the characteristics of the wall measured temperatures being without fluctuations.

4.2. Heat transfer coefficients and dryout

In Fig. 3, the experimental results for the mass velocities between 200 and 300 $kg\,m^{-2}\,s^{-1}$ for the microfin and plain tubes of 7 mm OD are presented. For the plain tube the heat transfer coefficient increases until a vapor quality near 65–75% when it begins to decrease because of dryout. On average, a very small effect of the mass velocity on the heat transfer coefficient is observed.

For the microfin tube the dryout phenomenon occurs for a vapor quality that increases with the mass velocity and for values near 63–78%. For $G = 300\ kg\,m^{-2}\,s^{-1}$, dryout occurs near a quality of 70% and 78% for the plain and microfin tube, respectively. For $G = 250\ kg\,m^{-2}\,s^{-1}$ dryout occurs in both tubes of 7 mm OD at 75% and for $G = 200\ kg\,m^{-2}\,s^{-1}$, quality dryout occurs at $x = 65$–70% in the plain tube and at $x = 62$–63% for the microfin tube. Even the results presented by Branescu [16], for 12.7 OD tubes, show dryout occurring at higher qualities for the microfin than the plain tube, as shown by Mori et al. [23], the number of experimental points are not enough to present a generalized and judicious conclusion about the dryout in these two tubes. For G values of 200 and 250 $kg\,m^{-2}\,s^{-1}$ there is no difference in the value of the heat transfer coefficient, which is higher for 300 $kg\,m^{-2}\,s^{-1}$.

This very minor influence of G on h was also observed by Kuo and Wang [15] for values of G equal to 100 and 200 $kg\,m^{-2}\,s^{-1}$ in a flow of R-407c inside a microfin tube with a diameter of 9.52 mm. For both tubes, the small increase of h with x and G can be attributed to the dominant effect of nucleate boiling in comparison with convective boiling. An analysis of the dominant mechanism in the annular flow as a function of the slopes of the experimental curves of h versus x was presented by Lallemand et al. [13].

These results show a general increase in the heat transfer coefficient of nearly 100% for the microfin tube compared with the plain tube, according of trends observed in [13,14].

The higher increase of 100% in h, when compared with the surface factor (= 1.46) (Table 1) means that the enhancement effect of the boiling caused by the microfins is not only due to an increase in the surface area but it is also caused by an increase in the number of nucleation sites.

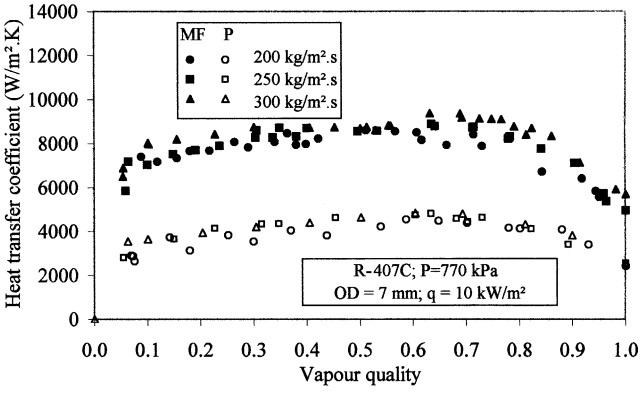

Fig. 3. Mass velocity effects for microfin and plain tubes.

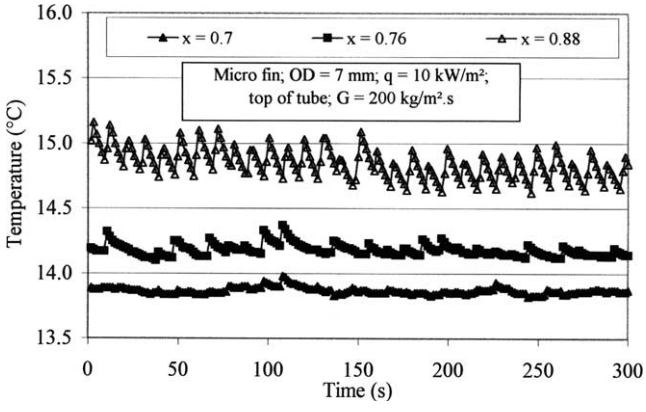

Fig. 4. Local wall temperature before and during dryout.

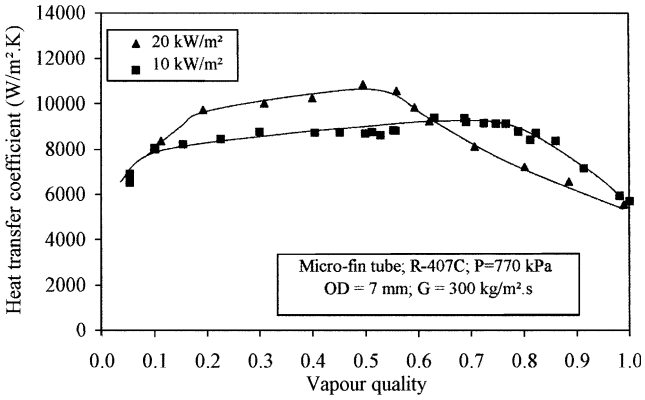

Fig. 5. Heat flux effect.

Fig. 4 presents the local wall temperature at the top of the wall as a function of time for three values of vapor quality: 0.70, 0.76 and 0.88, for the microfin 7 mm OD tube, for 10 $kW\,m^{-2}$ and 200 $kg\,m^{-2}\,s^{-1}$. For a vapor quality of 0.70 the wall temperature is nearly constant during the observed time interval and the dryout phenomenon has not yet started. For vapor qualities of 0.76 and 0.88 the wall temperature increases and shows oscillations indicating an intermittent dryout of the liquid film. Similar results were obtained at the bottom of the test section.

Fig. 5 shows the effect of the heat flux for the microfin tube with a 7 mm OD, for 10 and 20 $kW\,m^{-2}$ and for a mass velocity of 300 $kg\,m^{-2}\,s^{-1}$. A great reduction in the heat transfer coefficient indicates that the local dryout phenomenon occurs for vapor qualities near 80% and 55% for heat fluxes of 10 $kW\,m^{-2}$ and 20 $kW\,m^{-2}$, respectively. This expected trend in the results represents the general trend found in this work for the plain and microfin tubes.

For the vapor quality region between 0.15 and 0.53 the heat flux coefficients for 20 $kW\,m^{-2}$ are 19% higher than those for 10 $kW\,m^{-2}$. As in the case of Fig. 3, these results show that nucleate boiling plays an important role in the mechanism of heat transfer.

Fig. 6 shows the experimental heat transfer coefficient for microfin tubes of 7.0 and 12.7 mm OD for a heat flux and mass velocity of 10 $kW\,m^{-2}$ and 200 $kg\,m^{-2}\,s^{-1}$, respectively. The heat transfer coefficient for the 7.0 mm OD is higher than that for the 12.7 mm OD for a vapor quality less than 0.70, when it begins to reduce, indicating a dryout of the wall, whereas the heat transfer coefficient for the 12.7 mm OD continues to increase until the quality is 0.90, which can be considered as the quality for the beginning of the dryout for the 12.7 mm OD tube. The different slopes in the curves for each tube show that the dominant heat transfer mechanisms are those of nucleate boiling in the case of the 7 mm OD tube and of convective boiling in the case of the 12.7 mm OD tube. A more intensive convective heat transfer can be explained by the higher helix angle in the case of the 12.7 mm OD compared with the 7 mm OD which explains why the dryout phenomenon occurs for a very high vapor quality in the case of the larger diameter tube. However, the reasons for the different behaviors of the heat transfer coefficients for the low vapor qualities are not very clear in this work.

Unlike the result trends shown in Fig. 5, Seo and Kim [18] presented results showing a better heat transfer coefficient for 9.52 mm than for 7.00 mm OD fin tubes for internal convective boiling of R-22. As is indicated above, the effect of the higher twist angle for the 12.7 mm OD tube compared with the 7.0 mm OD tube could be one of the causes of the lower values for the heat transfer coefficient of the 12.7 mm tube. In fact, results presented by Thome [8] and Chamra et al. [14] show, for the same heat flux and the same tube diameter that there is a reduction in the heat transfer coefficient when the twist angle is high.

4.3. Pressure drop

Fig. 7 shows the pressure gradient as a function of the vapor quality for the four tubes tested in this work for a mass velocity of 200 $kg\,m^{-2}\,s^{-1}$ and for a heat flux of

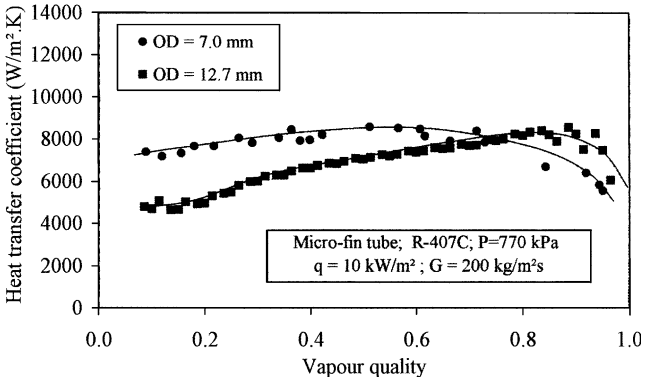

Fig. 6. Tube diameter effect.

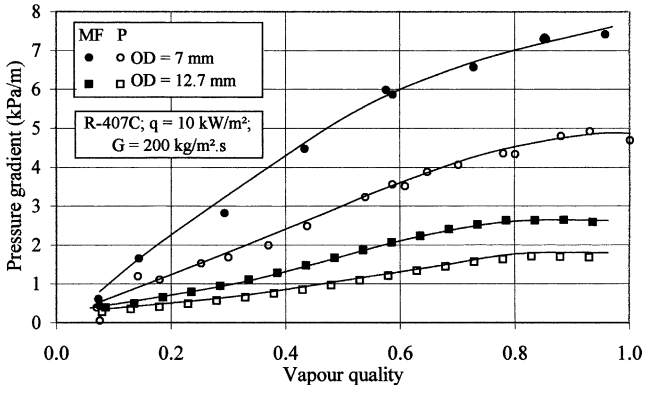

Fig. 7. Pressure gradient.

10 kW m^{-2}. In all cases the results show the expected trend of an increase in the pressure gradient as a function of the vapor quality. For the 7 mm OD tubes the average pressure drop ratios, computed by Eq. (5), are 3.01 and 4.98 kPa m^{-1} for the plain and microfin tubes, respectively, indicating a penalty coefficient of 1.65. In the case of the 12.7 mm OD tube the penalty coefficient is 1.66.

The efficiency index (Eq. (6)) for the test conditions with 200 kg m^{-2} s^{-1} and 10 kW m^{-2}, for R-407c are 1.21 and 1.51 for the 7 and 12.7 mm OD tubes, respectively.

5. Practical significance

The results and analysis presented in this work, particularly for the case with the heat flux of 10 kW m^{-2}, can be applied in the refrigeration industry because of the current interest to test the refrigerants chosen, in order to replace CFCs and HCFCs with HFC mixtures. Currently, the R-407c ternary zeotropic mixture is a possible alternative to replace R-22 in refrigerant systems. The utilization of microfin tubes can allow heat exchangers to become more compact.

6. Conclusions

The following conclusions are drawn from the present work. For tubes with OD = 7 mm, the heat transfer coefficient for the microfin tubes is higher (100%) than that for the plain tubes and the augmentation is greater than the increase in the heat transfer surface area of the microfin tubes when the surface factor is 1.46. For the microfin tube the dryout phenomenon occurs for a vapor quality that increases with the mass velocity and for values near 63–78%. For $G = 300$ kg m^{-2} s^{-1} dryout occurs for a corresponding vapor quality higher than that for the plain tube, 78% and 70%, respectively. However, this result was not verified for all the cases of G in this work and for $G = 250$ kg m^{-2} s^{-1} dryout occurs in both tubes of 7 mm OD at 75% and for $G = 200$ kg m^{-2} s^{-1}, the quality at which dryout occurs is higher for the plain tube than for the microfin tube. The reduced number of experimental points for the dryout phenomenon in this work does not allow the presentation of general conclusions. In fact, dryout inside microfin tubes continues to be a point little analyzed, may be because of the experimental difficulties inherent in this kind of study.

For the same diameter the local dryout occurs when vapor quality decreases with an increase of the heat flux. For a heat flux and mass velocity of 10 kW m^{-2} and 200 kg m^{-2} s^{-1}, respectively, dryout occurs at lower vapor quality in the case of 7 mm OD tube compared with 12.7 mm OD tube. The results show a greater trend towards a dominant effect of the nucleate boiling in the case of 7 mm OD tube compared with 12.7 mm OD tube.

The pressure gradient increases as a function of the vapor quality.

References

[1] W.F. Stoecker, Refrigerants, in: Industrial Refrigeration Handbook, McGraw-Hill, 1998 (Ch. 12).
[2] R. Koster, G. Herres, P. Kaupmann, P. Hübner, Influence of the heat flux in mixture boiling: experiments and correlations, International Journal of Refrigeration 20 (8) (1997) 598–605.
[3] D. Jung, Y. Song, B. Park, Performance of alternative refrigerants mixtures for HCFC22, International Journal of Refrigeration 23 (2000) 466–474.
[4] K. Stephan, Two-phase heat exchange for new refrigerants and their mixtures, International Journal of Refrigeration 18 (3) (1995) 198–209.
[5] D. Gorenflo, State of the art in pool boiling heat transfer of new refrigerants, International Journal of Refrigeration 24 (2001) 6–14.
[6] G.P. Celata, M. Cumo, T. Setaro, Forced convective boiling in binary mixtures, International Journal of Heat Mass Transfer 36 (13) (1993) 3299–3309.
[7] R.L. Webb, Principles of Enhanced Heat Transfer, John Wiley and Sons, New York, 1994.
[8] J.R. Thome, Enhanced Boiling Heat Transfer, Hemisphere Publishing Corporation, New York, 1990.
[9] S. Kakaç, H. Liu, Heat Exchangers: Selection, Rating and Thermal Design, CRC Press, 1998.
[10] J.G. Collier, J.R. Thome, Convective Boiling and Condensation, 3rd ed., Clarendon Press, Oxford, 1996.
[11] V.P. Carey, Liquid–Vapor Phase-Change Phenomena, Taylor and Francis, Bristol, England, 1992.
[12] G.F. Hewitt, Boiling, in: W.R. Rohsenow, J.P. Hartnett, Y.I. Cho (Eds.), Handbook of Heat Transfer, 3rd ed., McGraw-Hill, 1998 (Ch. 15).
[13] M. Lallemand, C.N. Branescu, P. Haberschill, Coefficients d'échange locaux au cours de l' ébullition du R22 et du R407C dans des tubes horizontaux, lisse ou micro-aileté, International Journal of Refrigeration 24 (2001) 57–72.
[14] L.M. Chamra, R.L. Webb, M.R. Randlett, Advance micro-fin tubes for evaporation, International Journal of Heat and Mass Transfer 39 (9) (1996) 1827–1838.
[15] C.S. Kuo, C. Wang, Horizontal flow boiling of R-22 and R-407C in 9.52 mm micro-fin tube, Applied Thermal Engineering 16 (8/9) (1996) 719–731.
[16] C.N. Branescu, Ebullition en convection forcée du R22 e du R407C à l'intérieur de tubes horizontaux lisses et micro-ailetés, PhD thesis, in French, Institut National des Sciences Appliquées de Lyon, France, 2000.
[17] H. Ross, R. Radermacher, M. di Marzo, D. Didion, Horizontal flow boiling of pure and mixed refrigerants, International Journal of Heat and Mass Transfer 30 (1987) 979–992.
[18] K. Seo, Y. Kim, Evaporation heat transfer and pressure drop of R-22 in 7 and 9.52 mm smooth/micro-fin tubes, International Journal of Heat and Mass Transfer 43 (2000) 2869–2882.
[19] V.V. Klimenko, A generalized correlation for two-phase forced flow heat transfer, International Journal of Heat and Mass Transfer 31 (3) (1988) 541–552.
[20] V.V. Klimenko, A generalized correlation for two-phase forced flow heat transfer—second assessment, International Journal of Heat and Mass Transfer 33 (10) (1990) 2073–2088.
[21] G.B. Wallis, One Dimensional Two-Phase Flow, McGraw-Hill, 1969.

[22] Z. Liu, R.H.S. Winterton, A general correlation for saturated and subcooled flow boiling in tubes and annuli, based on a nucleate pool boiling equation, International Journal of Heat and Mass Transfer 34 (11) (1991) 2759–2766.
[23] H. Mori, S. Yoshida, K. Ohishi, Y. Kakimoto, Dryout quality and post-dryout heat transfer coefficient in horizontal evaporator tubes, in: E.W.P. Hahne (Ed.), 3rd European Thermal Sciences Conference 2000, 2000, pp. 839–844.
[24] National Institute of Standards and Technology (NIST), REFPROP—Thermodynamic and Transport Properties of Refrigerants and Refrigerant Mixtures, Standard Reference Database 23-Version 6.0, 1998, USA.
[25] L. Zhang, E. Hihara, T. Saito, J. Taek-Oh, Boiling heat transfer of a ternary refrigerant mixture inside a horizontal smooth tube, International Journal of Heat Mass Transfer 40 (1997) 2009–2017.
[26] N. Kattan, Contribution to the heat transfer analysis of substitute refrigerants in evaporator tubes or enhanced tube surfaces, PhD thesis, Ecole Polytechnique Fédérale de Lausanne, Switzerland, 1996.
[27] N. Kattan, J.R. Thome, D. Favrat, Flow boiling in horizontal tubes: Part 1—Development of a diabatic two-phase flow pattern map, Transactions of the ASME-Journal of Heat Transfer 120 (1998) 140–147.
[28] S.J. Kline, The purposes of uncertainty analysis, ASME Journal of Fluid Engineering 107 (1985) 153–160.
[29] J.P. Holman, Experimental Methods for Engineers, McGraw-Hill, New York, 1989.